
Sensitivity Analysis for Climate Science with Generative Flow Models

Alex Dobra*

Dept. of Engineering
University of Oxford

Jakiw Pidstrigach

Dept. of Statistics
University of Oxford

Tim Reichelt

Dept. of Physics
University of Oxford

Paolo Fraccaro

IBM Europe

Johannes Jakubik

IBM Europe

Anne Jones

IBM Europe

Christian Schroeder de Witt

Dept. of Engineering
University of Oxford

Philip Stier

Dept. of Physics
University of Oxford

Philip Torr

Dept. of Engineering
University of Oxford

Abstract

Sensitivity analysis is a cornerstone of climate science, essential for understanding phenomena ranging from storm intensity to long-term climate feedbacks. However, computing these sensitivities using traditional physical models is often prohibitively expensive in terms of both computation and development time. While modern AI-based generative models are orders of magnitude faster to evaluate, computing sensitivities with them remains a significant bottleneck. This work addresses this challenge by applying the adjoint state method for calculating gradients in generative flow models, with diffusion models as a special case. We apply this method to the cBottle generative model, an emulator of ERA5 data, to perform sensitivity analysis with respect to sea surface temperatures. Furthermore, we propose a novel gradient self-consistency check to quantitatively validate the computed sensitivities against the model’s own outputs. Our results provide initial evidence that this approach can produce reliable gradients, reducing the computational cost of sensitivity analysis from weeks on a supercomputer with a physical model to hours on a GPU, thereby simplifying a critical workflow in climate science.

1 Introduction

Sensitivity analysis is widely applied throughout climate science, e.g. for investigating the drivers of storms [1], the importance of observations [2] or understanding climate feedbacks [3, 4]. However, conducting sensitivity analysis with classical physical simulation models is prohibitively expensive, relying either on deriving and implementing adjoints by hand [5, 6, 7] or running finite difference approximations [3]. For example, a standard approach for estimating the response of the atmosphere to spatial changes in temperature fields relies on Green’s function method which requires executing an expensive General Circulation Model (GCM) for thousands of model years which can take weeks, even on a supercomputer [8, 9, 10, 11, 12, 3, 4].

Recently, there has been an explosion of development of large AI models for weather and climate. While expensive to train, they are significantly faster and differentiable by default, warranting an investigation into their potential to simplify the sensitivity analysis workflow. Modern AI models

*Corresponding author: alex.dobra@robots.ox.ac.uk

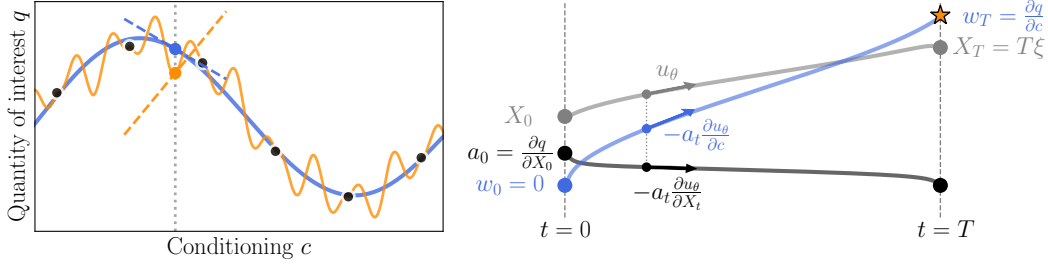


Figure 1: **Left.** An illustration of how an overfit model (orange) has uninformative gradients when compared to a well-fit model (blue). Our experiments show that cBottle is more of the latter than the former, encouraging its use for SST sensitivity analysis. **Right.** A sketch of the adjoint sensitivity method in the EDM parametrization. Given the generated vector X_0 and a function to obtain the quantity of interest, $q(X_0)$, we obtain the desired sensitivity $\frac{\partial q}{\partial c}$ by propagating X_t , the adjoint a_t and the gradient w_t through their respective ODEs.

are developed in frameworks like PyTorch [13] and JAX [14], which are equipped with automatic differentiation (AD) engines [15]. Consequently, obtaining the gradient of any scalar quantity derived from the model’s output with respect to any model input only requires a single function call to the AD engine, which has motivated their use for initial condition sensitivity studies [1, 16, 17].

Notably, flow and diffusion models [18, 19, 20, 21] have gained popularity in weather and climate due to their powerful generative properties and their ability to model uncertainty. Diffusion models have demonstrated state-of-the-art results in weather forecasting [22] and are able to reproduce atmospheric states [23]. The method presented in this paper provides a way to extract gradients from these types of models, reducing the cost of sensitivity analysis from days to weeks on a supercomputer to minutes or hours on a GPU. However, it is not as clear if these models can produce informative gradients even if they provide a good fit to the data, see Figure 1 for an illustration of this problem. To begin the work of evaluating their quality, this paper introduces a method of extracting gradients from flow models and checking their consistency with model predictions through finite differences.

2 Background and notation

Climate in a Bottle. The experiments in this work are done with the simplest Climate in a Bottle diffusion model [23] (henceforth called cBottle). Given the day of year τ , second of day ζ , sea surface temperature forcing c , and a high dimensional random vector ξ , the cBottle model generates 45 atmospheric variables (4 3D variables on 8 pressure levels, 6 column variables and 7 surface variables) at a ground resolution of ~ 100 km. See App. C for details. cBottle has been trained on both ERA5 reanalysis data [24] and outputs from the ICON climate model [25], providing a unique test-bed for gradient extraction methods. While the empirical results are computed with cBottle, the method presented here is not specific to cBottle and applies to generative flow models in general.

Flow models. Diffusion models [18, 19, 20], and the more recent flow matching [21, 26, 27] are all special cases of flow models, a family of generative models which learn a time-varying velocity field $u_\theta(X_t, t)$ that transports an easy-to-sample probability distribution p_{init} to a data probability distribution p_{data} . In what follows, we will use the parameterization of the Elucidated Diffusion Model (EDM) [28] with deterministic sampling.

Conditioning. Flow models can be guided by input variables c to sample from the conditional distribution $p_{data}(\cdot|c)$ [29, 30, 31]. Therefore, the procedure for generation implies sampling ξ from the standard Gaussian, picking a conditioning variable c and solving the ODE

$$dX_t = u_\theta(X_t, t, c)dt, \text{ with } X_T = T\xi \text{ and } \xi \sim \mathcal{N}(0, \text{Id})$$

backwards in time, from T to 0, obtaining the generated sample $X_0 \sim p_{data}(\cdot|c)$.

3 Methods

We are interested in a scalar quantity derived from a generated sample $q(X_0)$ and how this quantity varies with conditioning $\frac{\partial q}{\partial c}$. For example, in the context of cBottle, q can be net outgoing radiation

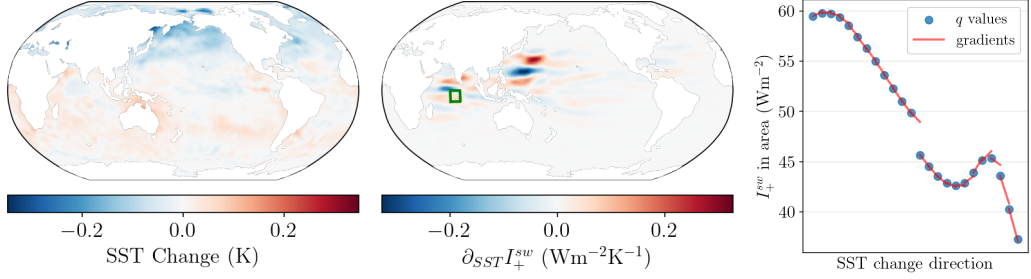


Figure 2: A qualitative example for the gradient self-consistency check. Pick a quantity of interest q , in this case the average top of the atmosphere outgoing shortwave radiation (I_+^{sw}) in a patch of the Indian Ocean (green rectangle). Pick an SST change vector δc , add it to the current c , and calculate the new $q(c + \delta c)$ and the gradient $\frac{\partial q}{\partial c}(c + \delta c)$. Repeating this procedure shows that, in the δc direction, q is mostly a smooth function with sensible gradients.

globally, precipitation on the coast of Peru or wind shear in the tropical Pacific, and c is global sea surface temperatures. As flow models have very deep computational graphs due to the recurrent calls to the model, it is not feasible to simply use AD to obtain this derivative. We first write down a continuous counterpart of the chain-rule

$$\frac{\partial q}{\partial c} = \frac{\partial q}{\partial X_0} \frac{\partial X_0}{\partial c} = \frac{\partial q}{\partial X_0} \int_T^0 \frac{\partial X_0}{\partial X_t} \frac{\partial u_\theta}{\partial c}(X_t, t, c) dt.$$

The key step is to use the adjoint state $a_t = \frac{\partial q}{\partial X_0} \frac{\partial X_0}{\partial X_t}$, which satisfies the ODE

$$\frac{d}{dt} a_t = -a_t \frac{\partial u_\theta}{\partial X_t}.$$

Letting $w_{T-t} = a_t \frac{\partial X_t}{\partial c}$ we see the desired result is $\frac{\partial q}{\partial c} = a_0 \frac{\partial X_0}{\partial c} = w_T$. Solving the system of ODEs

$$\frac{d}{dt} \begin{bmatrix} X_t \\ a_t \\ w_t \end{bmatrix} = \begin{bmatrix} u_\theta \\ -a_t \frac{\partial u_\theta}{\partial X_t} \\ -a_t \frac{\partial u_\theta}{\partial c} \end{bmatrix}, \text{ with } \begin{bmatrix} X_0 \\ a_0 \\ w_0 \end{bmatrix} = \begin{bmatrix} X_0 \\ \frac{\partial q}{\partial X_0} \\ 0 \end{bmatrix}, \quad (1)$$

from 0 to T yields $\frac{\partial q}{\partial c} = w_T$. The process is depicted in the right panel of Figure 1, and proofs can be found in [32, 33, 34].

Gradient self-consistency check. The approximate nature of the flow model mapping from c to X_0 means the reliability of its gradients is not immediately clear, see Figure 1. While the model’s outputs are typically validated for consistency against real-world data or physical models [23], the trustworthiness of the gradients is commonly not assessed. We bridge this gap by proposing a self-consistency check that validates the model’s gradients against its own outputs, thereby using the validation of the predictive samples to establish confidence in the model gradients. Let a finite difference in model input be δc . For small enough δc and smooth q , the following approximation should hold:

$$\frac{1}{2} \left(\frac{\partial q}{\partial c}(c) + \frac{\partial q}{\partial c}(c + \delta c) \right) \cdot \delta c \approx q(c + \delta c) - q(c). \quad (2)$$

Plugging these two expressions into a selected similarity metric, we can obtain a quantitative measure of the self-consistency of gradients.

ODE directional gradient propagation. While the above should confirm the correctness of the adjoint method, it is not feasible to quantitatively evaluate the gradient consistency for the entire model output, as we have to run the algorithm one scalar q at a time. To do gradient self-consistency checks at scale, we use the following insight: finite difference calculations require an *a priori* direction δc in which the gradients are evaluated. This motivates the use of a different method for quickly probing gradients, detailed in Appendix A.

4 Results with Climate in a Bottle

We conduct our experiments with cBottle, a diffusion model of the EDM type [28]. It can be easily reparameterized as a flow model $dX_t = u_\theta(X_t, t, c, \tau, \zeta)dt$, with $X_T = T\xi$ and $\xi \sim \mathcal{N}(0, \text{Id})$ via

the probability flow ODE [20]. The conditioning variables are c – sea surface temperature (SST) forcing, τ – day of the year and ζ – UTC second of day. For now, we let c vary, but we keep τ , ζ and ξ constant.

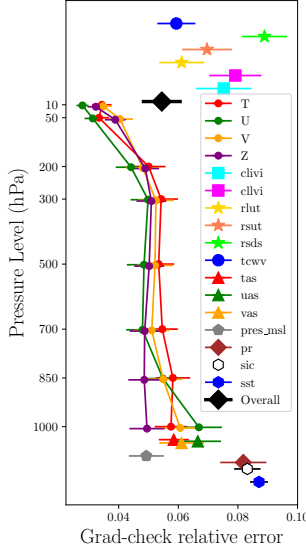


Figure 3: Grad-check relative errors for all 45 variables generated by cBottle (see App. C.1). Lower is better.

The results of this specific experiment seem to suggest that variables higher in the atmosphere have better gradients. Further investigation reveals that their connection to SSTs is weaker compared to variables lower in the atmosphere, which most likely means they are a “smoother” function of SSTs. This leads to lower grad-check errors, as the approximation in equation 2 becomes more accurate. This is confirmed by ablation experiments where the finite difference δc is reduced, see Appendix A.3.

5 Discussion and future work

Limitations. While the results in this paper are promising and suggest that cBottle has self-consistent gradients, large-scale grad-check experiments have not been conducted. Moreover, there is no guarantee that the sensitivities extracted from the model make physical sense, especially with out-of-distribution conditioning, like SSTs expected due to climate change (see Appendix C.2).

Future work. Studies on the physical correctness of gradients must be performed, both with the presented algorithm and its extension to seasonal sensitivity analysis (B). To get a representative value of any sensitivity and its uncertainties, we need to compute the mean and variance of $\frac{\partial q}{\partial c}$ over the random vector ξ . The gradients will need to be further averaged over different times of day ζ to include different weather states across the globe, and perhaps neighboring values of SSTs c and day of year τ , for a fuller picture of the gradients’ behavior in a certain month or season.

A promising avenue for greatly extending the applications of this method is model guidance. To condition the model to generate desired weather states from the exact posterior (for example, show a realistic hurricane in the Atlantic), we can train a separate model [29, 30, 31] that uses a guiding variable $y = G(X_0)$, where G is an observation operator. Gradients with respect to y can then be pulled through the small guiding model. This method would allow calculations of gradients of anything with respect to anything, including variables not included in the original model, for example CO₂ concentrations, aerosol optical depths or ocean salinity.

References

- [1] Jorge Baño-Medina, Ankur Sengupta, James D. Doyle, et al. Are ai weather models learning atmospheric physics? a sensitivity analysis of cyclone xynthia. *npj Climate and Atmospheric Science*, 8(92), 2025.
- [2] Ryan D Torn and Gregory J Hakim. Ensemble-based sensitivity analysis. *Monthly Weather Review*, 136(2):663–677, 2008.
- [3] Jonah Bloch-Johnson, Maria AA Rugenstein, Marc J Alessi, Cristian Proistosescu, Ming Zhao, Bosong Zhang, Andrew IL Williams, Jonathan M Gregory, Jason Cole, Yue Dong, et al. The green’s function model intercomparison project (gfmip) protocol. *Journal of Advances in Modeling Earth Systems*, 16(2):e2023MS003700, 2024.
- [4] Senne Van Loon, Maria Rugenstein, and Elizabeth A Barnes. Reanalysis-based global radiative response to sea surface temperature patterns: Evaluating the ai2 climate emulator. *Geophysical Research Letters*, 52(14):e2025GL115432, 2025.
- [5] Ronald M Errico. What is an adjoint model? *Bulletin of the American Meteorological Society*, 78(11):2577–2592, 1997.
- [6] Yannick Trémolet. Model-error estimation in 4d-var. *Quarterly Journal of the Royal Meteorological Society: A journal of the atmospheric sciences, applied meteorology and physical oceanography*, 133(626):1267–1280, 2007.
- [7] James D Doyle, Clark Amerault, Carolyn A Reynolds, and P Alex Reinecke. Initial condition sensitivity and predictability of a severe extratropical cyclone using a moist adjoint. *Monthly Weather Review*, 142(1):320–342, 2014.
- [8] Grant Branstator. Analysis of general circulation model sea-surface temperature anomaly simulations using a linear model. part i: Forced solutions. *Journal of Atmospheric Sciences*, 42(21):2225–2241, 1985.
- [9] Mark Holzer and Timothy M Hall. Transit-time and tracer-age distributions in geophysical flows. *Journal of the atmospheric sciences*, 57(21):3539–3558, 2000.
- [10] Joseph J Barsugli and Prashant D Sardeshmukh. Global atmospheric sensitivity to tropical sst anomalies throughout the indo-pacific basin. *Journal of Climate*, 15(23):3427–3442, 2002.
- [11] Chen Zhou, Mark D Zelinka, and Stephen A Klein. Analyzing the dependence of global cloud feedback on the spatial pattern of sea surface temperature change with a green’s function approach. *Journal of Advances in Modeling Earth Systems*, 9(5):2174–2189, 2017.
- [12] Yue Dong, Cristian Proistosescu, Kyle C Armour, and David S Battisti. Attributing historical and future evolution of radiative feedbacks to regional warming patterns using a green’s function approach: The preeminence of the western pacific. *Journal of Climate*, 32(17):5471–5491, 2019.
- [13] Adam Paszke, Sam Gross, Francisco Massa, Adam Lerer, James Bradbury, Gregory Chanan, Trevor Killeen, Zeming Lin, Natalia Gimelshein, Luca Antiga, Alban Desmaison, Andreas Kopf, Edward Yang, Zachary DeVito, Martin Raison, Alykhan Tejani, Sasank Chilamkurthy, Benoit Steiner, Lu Fang, Junjie Bai, and Soumith Chintala. Pytorch: An imperative style, high-performance deep learning library. In *Advances in Neural Information Processing Systems 32*, pages 8024–8035. Curran Associates, Inc., 2019.
- [14] James Bradbury, Roy Frostig, Peter Hawkins, Matthew James Johnson, Chris Leary, Dougal Maclaurin, George Necula, Adam Paszke, Jake VanderPlas, Skye Wanderman-Milne, and Qiao Zhang. JAX: composable transformations of Python+NumPy programs, 2018.
- [15] Atilim Gunes Baydin, Barak A Pearlmutter, Alexey Andreyevich Radul, and Jeffrey Mark Siskind. Automatic differentiation in machine learning: a survey. *Journal of machine learning research*, 18(153):1–43, 2018.

[16] P Trent Vonich and Gregory J Hakim. Predictability limit of the 2021 pacific northwest heatwave from deep-learning sensitivity analysis. *Geophysical Research Letters*, 51(19):e2024GL110651, 2024.

[17] Kinya Toride, Matthew Newman, Andrew Hoell, Antonietta Capotondi, Jakob Schlör, and Dillon J Amaya. Using deep learning to identify initial error sensitivity for interpretable enso forecasts. *Artificial Intelligence for the Earth Systems*, 4(2):e240045, 2025.

[18] Jascha Sohl-Dickstein, Eric Weiss, Niru Maheswaranathan, and Surya Ganguli. Deep unsupervised learning using nonequilibrium thermodynamics. In *International Conference on Machine Learning*, pages 2256–2265, 2015.

[19] Jonathan Ho, Ajay Jain, and Pieter Abbeel. Denoising diffusion probabilistic models. In *Advances in Neural Information Processing Systems*, 2020.

[20] Yang Song, Jascha Sohl-Dickstein, Diederik P Kingma, Abhishek Kumar, Stefano Ermon, and Ben Poole. Score-based generative modeling through stochastic differential equations. In *International Conference on Learning Representations*, 2021.

[21] Yaron Lipman, Ricky T. Q. Chen, Haggai Ben-Hamu, Maximilian Nickel, and Matthew Le. Flow matching for generative modeling. In *International Conference on Learning Representations*, 2023.

[22] Ilan Price, Alvaro Sanchez-Gonzalez, Ferran Alet, Tom R. Andersson, Andrew El-Kadi, Dominic Masters, Timo Ewalds, Jacklynn Stott, Shakir Mohamed, Peter Battaglia, Remi Lam, and Matthew Willson. Probabilistic weather forecasting with machine learning. *Nature*, 637(8044):84–90, 2025.

[23] Noah D. Brenowitz, Tao Ge, Akshay Subramaniam, Peter Manshausen, Aayush Gupta, David M. Hall, Morteza Mardani, Arash Vahdat, Karthik Kashinath, and Michael S. Pritchard. Climate in a bottle: Towards a generative foundation model for the kilometer-scale global atmosphere, 2025.

[24] Hans Hersbach, Bill Bell, Paul Berrisford, Shoji Hirahara, András Horányi, Joaquín Muñoz-Sabater, Julien Nicolas, Carole Peubey, Raluca Radu, Dinand Schepers, et al. The era5 global reanalysis. *Quarterly journal of the royal meteorological society*, 146(730):1999–2049, 2020.

[25] Cathy Hohenegger, Peter Korn, Leonidas Linardakis, René Redler, Reiner Schnur, Panagiotis Adamidis, Jiawei Bao, Swantje Bastin, Milad Behravesh, Martin Bergemann, et al. Icon-sapphire: simulating the components of the earth system and their interactions at kilometer and subkilometer scales. *Geoscientific Model Development*, 16(2):779–811, 2023.

[26] Xingchao Liu, Chengyue Gong, and Qiang Liu. Flow straight and fast: Learning to generate and transfer data with rectified flow, 2022.

[27] Michael S. Albergo and Eric Vanden-Eijnden. Stochastic interpolants: A unifying framework for flows and diffusions. In *Advances in Neural Information Processing Systems*, 2023.

[28] Tero Karras, Miika Aittala, Timo Aila, and Samuli Laine. Elucidating the design space of diffusion-based generative models. In *Advances in Neural Information Processing Systems*, 2022.

[29] Lvmin Zhang, Anyi Rao, and Maneesh Agrawala. Adding conditional control to text-to-image diffusion models. In *ICCV*, pages 3813–3824. IEEE, 2023.

[30] Alexander Denker, Francisco Vargas, Shreyas Padhy, Kieran Didi, Simon V Mathis, Riccardo Barbano, Vincent Dutordoir, Emile Mathieu, Urszula Julia Komorowska, and Pietro Lio. DEFT: Efficient fine-tuning of diffusion models by learning the generalised $\$h\$$ -transform. In *The Thirty-eighth Annual Conference on Neural Information Processing Systems*, 2024.

[31] Jakiw Pidstrigach, Elizabeth Louise Baker, Carles Domingo-Enrich, George Deligiannidis, and Nikolas Nüsken. Conditioning diffusions using malliavin calculus. In *Forty-second International Conference on Machine Learning*, 2025.

- [32] Lev Semenovich Pontryagin, E. F. Mishchenko, V. G. Boltyanskii, and R. V. Gamkrelidze. *The Mathematical Theory of Optimal Processes*. Interscience Publishers, New York, 1962.
- [33] Ricky T. Q. Chen, Yulia Rubanova, Jesse Bettencourt, and David Duvenaud. Neural ordinary differential equations. In *Proceedings of the 32nd International Conference on Neural Information Processing Systems*, NIPS’18, page 6572–6583, Red Hook, NY, USA, 2018. Curran Associates Inc.
- [34] Ilya V. Schurov. Adjoint state method, backpropagation and neural odes, August 5 2022. Accessed on 2025-08-19.

A ODE directional gradient propagation

Solving the ODE system

$$\frac{d}{dt} \begin{bmatrix} X_t \\ v_t \end{bmatrix} = \begin{bmatrix} u_\theta(X_t, t, c) \\ \frac{\partial u_\theta}{\partial X_t}(X_t, t, c)v_t + \frac{\partial u_\theta}{\partial c}(X_t, t, c)\delta c \end{bmatrix}, \text{ with } \begin{bmatrix} X_T \\ v_T \end{bmatrix} = \begin{bmatrix} T\xi \\ 0 \end{bmatrix}. \quad (3)$$

from T to 0 yields the desired directional derivative $v_0 = \frac{\partial X_0}{\partial c}\delta c$ in the δc direction. Choosing the L1-norm as a measure of model’s gradient consistency, we can write down the grad-check metric GC :

$$GC(X_0, c, \delta c) = \left\| \frac{1}{2} \left(\frac{\partial X_0}{\partial c}(c)\delta c + \frac{\partial X_0}{\partial c}(c + \delta c)\delta c \right) - (X_0(c + \delta c) - X_0(c)) \right\|_1. \quad (4)$$

A.1 Proof

Starting from the ODE

$$\frac{d}{dt} X_t = u_\theta(X_t, t, c)$$

take the partial derivative $\frac{\partial}{\partial c}$ while keeping θ and t constant

$$\frac{d}{dt} \left(\frac{\partial X_t}{\partial c} \right)_{\theta, t} = \left(\frac{\partial u_\theta}{\partial c} \right)_{\theta, t} = \left(\frac{\partial u_\theta}{\partial X_t} \right)_{\theta, t, c} \left(\frac{\partial X_t}{\partial c} \right)_{\theta, t} + \left(\frac{\partial u_\theta}{\partial c} \right)_{\theta, t, X_t},$$

where we have used the fact that the derivative operators $\frac{d}{dt}$ and $(\partial_c)_{\theta, t}$ commute. Letting $h_t = \left(\frac{\partial X_t}{\partial c} \right)_{\theta, t}$ and neglecting to explicitly show what is kept constant in situations where everything is, we get

$$\frac{d}{dt} h_t = \frac{\partial u_\theta}{\partial X_t} h_t + \frac{\partial u_\theta}{\partial c}.$$

Instead of calculating the full Jacobians $\frac{\partial u_\theta}{\partial X_t}$ and $\frac{\partial u_\theta}{\partial c}$, which quickly becomes impossible in high-dimensional situations like image generation, we instead multiply the above equation by δc from the right and with another change of variables $v_t = h_t \delta c$, we obtain the desired ODE:

$$\frac{d}{dt} v_t = \frac{\partial u_\theta}{\partial X_t} v_t + \frac{\partial u_\theta}{\partial c} \delta c.$$

This method leverages the efficient Jacobian Vector Product algorithms of PyTorch or JAX to directly obtain $\frac{\partial u_\theta}{\partial X_t} v_t + \frac{\partial u_\theta}{\partial c} \delta c$ — this can be done at the additional cost of just one forward pass. Finally, it is clear that $v_T = \frac{\partial X_T}{\partial c} \delta c = 0$ as at the starting point the velocity field guided by c has not yet pushed X_T at all. Putting this together with the forward pass in the same ODE system yields equation 3.

Full derivative. We can also extend this to get the full derivative (see Appendix B):

$$\frac{d}{dt} \left(\frac{\partial X_t}{\partial c} \right)_{\theta, t} = \left(\frac{\partial u_\theta}{\partial X_t} \right)_{\theta, t, c, \tau} \left(\frac{\partial X_t}{\partial c} \right)_{\theta, t} + \left(\frac{\partial u_\theta}{\partial c} \right)_{\theta, t, X_t, \tau} + \left(\frac{\partial u_\theta}{\partial \tau} \right)_{\theta, t, X_t, c} \left(\frac{\partial \tau}{\partial c} \right)_{\theta, t},$$

which, multiplied from the right by δc , neglecting to explicitly write down what is kept constant when everything is, and using the expression for $\frac{\partial \tau}{\partial c}$ from Appendix B, yields

$$\frac{d}{dt} v_t = \frac{\partial u_\theta}{\partial X_t} v_t + \frac{\partial u_\theta}{\partial c} \delta c + \frac{\partial u_\theta}{\partial \tau} \frac{\tau_{i+1} - \tau_i}{c(\tau_{i+1}) - c(\tau_i)} \delta c.$$

A.2 Grad-check relative error metric

With the directional gradient method, we can form the grad-check metric for all generated variables at the same time. While this is a good way of probing the gradients of the whole model output, it does not guarantee self-consistency for any q , as $q(X_0)$ might be a highly non-smooth function of X_0 . Let $y = \Omega(X_0)$, a variable generated by cBottle (for example, outgoing long-wave radiation globally), where Ω is a simple slicing operator. The grad-check relative error metric for y is defined as

$$\text{RGC} = \frac{\mathbb{E}_{\xi, c, \delta c} \left\| \frac{1}{2} \left(\frac{\partial y}{\partial c}(c) \delta c + \frac{\partial y}{\partial c}(c + \delta c) \delta c \right) - (y(c + \delta c) - y(c)) \right\|_1}{\mathbb{E}_{\xi, c, \delta c} \|y(c + \delta c) - y(c)\|_1}.$$

Let's unpack this. The numerator is simply the two terms of equation 2 plugged into an L1-norm. The expectation is taken over the random vector ξ , to probe gradients of more and less likely weather states given the conditioning — although for a given pair of points, ξ should be the same for both, otherwise we would have to use a probabilistic metric like CRPS. We also take the expectation over the pair c and $c + \delta c$ to probe gradients at multiple points on the conditioning manifold and in different directions δc . In the case of cBottle and for an even more comprehensive metric, we should average over τ and ζ too.

The denominator acts as a normalization term, which allows comparison of the metric across different variables y . Not only does it make the metric unitless, but also counteracts the effects of some variables simply changing less than others on huge swaths of the globe — for example, in cBottle, sea ice fraction differences are always very small compared to other variables.

It is worth investigating new versions of this metric in future work, but the principles guiding the design of the current one seem sensible and should be reused.

We will now explain how the uncertainties in the RGC were calculated (the error-bars in Figure 3). As the RGC is a quotient of two random variables, we used the approximation

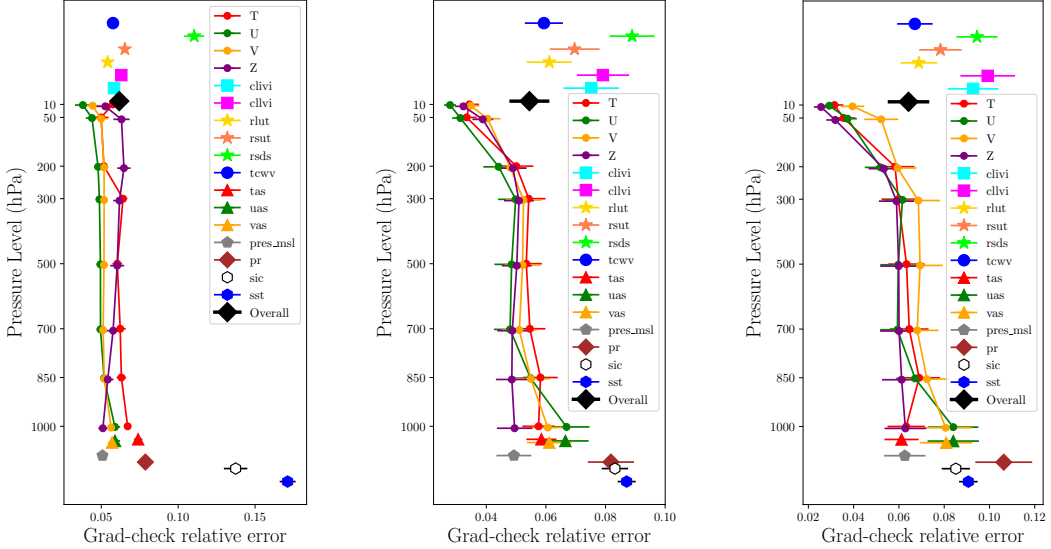
$$\text{Var}\left(\frac{X}{Y}\right) = \frac{1}{n \mathbb{E}[Y]^2} \left(\text{Var}(X) + \left(\frac{\mathbb{E}[X]}{\mathbb{E}[Y]} \right)^2 \text{Var}(Y) - 2 \frac{\mathbb{E}[X]}{\mathbb{E}[Y]} \text{Cov}(X, Y) \right),$$

where X and Y are two random variables and n is the number of samples used for the approximation.

For the “Overall” error, we have combined the standard deviations (square root of the above variance) in quadrature, as if the variables are independent, except for the profile variables, where high correlation was apparent — we just reduced the weight of their RGC standard deviation values in the quadrature combination.

A.3 Ablations

See Figure 4.



(a) Grad-check relative errors with a step size δc corresponding to SST change in 11h in October 2021.

(b) Grad-check relative errors with a step size δc corresponding to SST change in 24h in October 2021. Same as Figure 2.

(c) Same as (b), but we have used the seasonal sensitivity algorithm (the full derivative), as described in Appendix B.

Figure 4: As mentioned in the main text, the trend of variables in the upper atmosphere seemingly having worse gradients disappears once we decrease the step-size δc , compare (a) to (b). This also highlights the limitations of the grad-check relative error metric (A.2), as some variables that change very little in large parts of the globe (like sea ice fraction and SST) tend to have higher relative errors due to normalization. In (c) we also show the performance of the full derivative algorithm, which is slightly worse than the control (b), most likely due to discretization errors — this requires further investigation.

B Getting full derivatives with the adjoint sensitivity method

In the case in which the inputs to the flow model are dependent on each other, as is the case with cBottle’s forcing SSTs c and day of year τ , we might be interested in total derivatives, in addition to the partial derivatives obtainable through the adjoint sensitivity method. To reiterate, obtaining partial derivatives (from a velocity-reparameterized EDM) with the adjoint sensitivity method implies solving the system of ODEs

$$\frac{d}{dt} \begin{bmatrix} X_t \\ a_t \\ w_t \\ v_t \end{bmatrix} = \begin{bmatrix} u_\theta \\ -a_t \frac{\partial u_\theta}{\partial X_t} \\ -a_t \frac{\partial u_\theta}{\partial c} \\ -a_t \frac{\partial u_\theta}{\partial \tau} \end{bmatrix}, \text{ with } \begin{bmatrix} X_0 \\ a_0 \\ w_0 \\ v_0 \end{bmatrix} = \begin{bmatrix} X_0 \\ \frac{\partial q}{\partial X_0} \\ 0 \\ 0 \end{bmatrix}$$

from $t = 0$ to $t = T$, where $w_T = \frac{\partial q}{\partial c}$ and $v_T = \frac{\partial q}{\partial \tau}$. In practice, calculating the additional derivative $\frac{\partial u_\theta}{\partial \tau}$ adds negligible computational cost, as the backpropagation process through the computational graph happens the same way and with the same starting tangent $-a_t$. The total derivative is then

$$\frac{dq}{dc} = \frac{\partial q}{\partial c} + \frac{\partial q}{\partial \tau} \frac{\partial \tau}{\partial c} = w_T + v_T \frac{\partial \tau}{\partial c}.$$

In the case of cBottle, we know that $c(\tau)$ is linearly interpolated between the nearest two mid-month monthly mean SSTs (see Appendix C.2)

$$c(\tau) = c(\tau_i) + \frac{\tau - \tau_i}{\tau_{i+1} - \tau_i} (c(\tau_{i+1}) - c(\tau_i)),$$

and so

$$\frac{\partial \tau}{\partial c} = \left(\frac{\partial c}{\partial \tau} \right)^{-1} = \frac{\tau_{i+1} - \tau_i}{c(\tau_{i+1}) - c(\tau_i)}.$$

Otherwise, a more general method of approximating $\frac{\partial \tau}{\partial c}$ is to train a regressor and to get this gradient with an AD call.

C cBottle details

C.1 Generated variables

See Table 1.

Short name	Description	Units
Profile variables @ 1000, 850, 700, 500, 300, 200, 50, 10 hPa		
T	air temperature (profile)	K
U	zonal wind (profile)	m s^{-1}
V	meridional wind (profile)	m s^{-1}
Z	geopotential height	m
Column variables		
clivi	column integrated cloud ice	kg m^{-2}
cllvi	column integrated cloud water	kg m^{-2}
rlut	TOA outgoing longwave radiation	W m^{-2}
rsut	TOA outgoing shortwave radiation	W m^{-2}
rsds	surface downwelling shortwave radiation	W m^{-2}
tcvw	column integrated water vapour	kg m^{-2}
Surface variables		
pr	precipitation flux	$\text{kg m}^{-2} \text{s}^{-1}$
pres_msl	mean sea level pressure	Pa
sic	sea ice concentration (fractional)	—
sst	sea surface temperature	K
tas	2m air temperature	K
uas	zonal wind at 10m	m s^{-1}
vas	meridional wind at 10m	m s^{-1}

Table 1: Variables grouped into profile, column, and surface categories with their ICON names, descriptions, and units.

C.2 The nature of SST conditioning data

As mentioned in the results section, cBottle is using one of its conditioning variables, the day of year τ , to obtain the sea surface temperature forcing $c(\tau)$. This procedure is mentioned but not detailed in their paper, and so we will describe here. They use the AMIP dataset `input4MIPs.CMIP6Plus.CMIP.PCMDI.PCMDI-AMIP-1-1-9.ocean.mon.tosbcs.g` which can be downloaded with a script from here. This dataset contains the estimated global mid-month, monthly mean SST from January 1870 to December 2022, all dated on the 16th of the month (except February, which has the 15th). If the model is given a day of year τ , $c(\tau)$ is linearly interpolated from the nearest two data points:

$$c(\tau) = c(\tau_i) + \frac{\tau - \tau_i}{\tau_{i+1} - \tau_i} (c(\tau_{i+1}) - c(\tau_i)),$$

where τ_i is the mid-month day-of-year of month i and τ satisfies $\tau_i \leq \tau < \tau_{i+1} < \tau + 31$.

For simplicity, we have maintained that τ is the day of the year, but it would be more precise to say it is the day of the year plus the day fraction: $\tau = 1.5$ means January 1st 12:00 UTC.

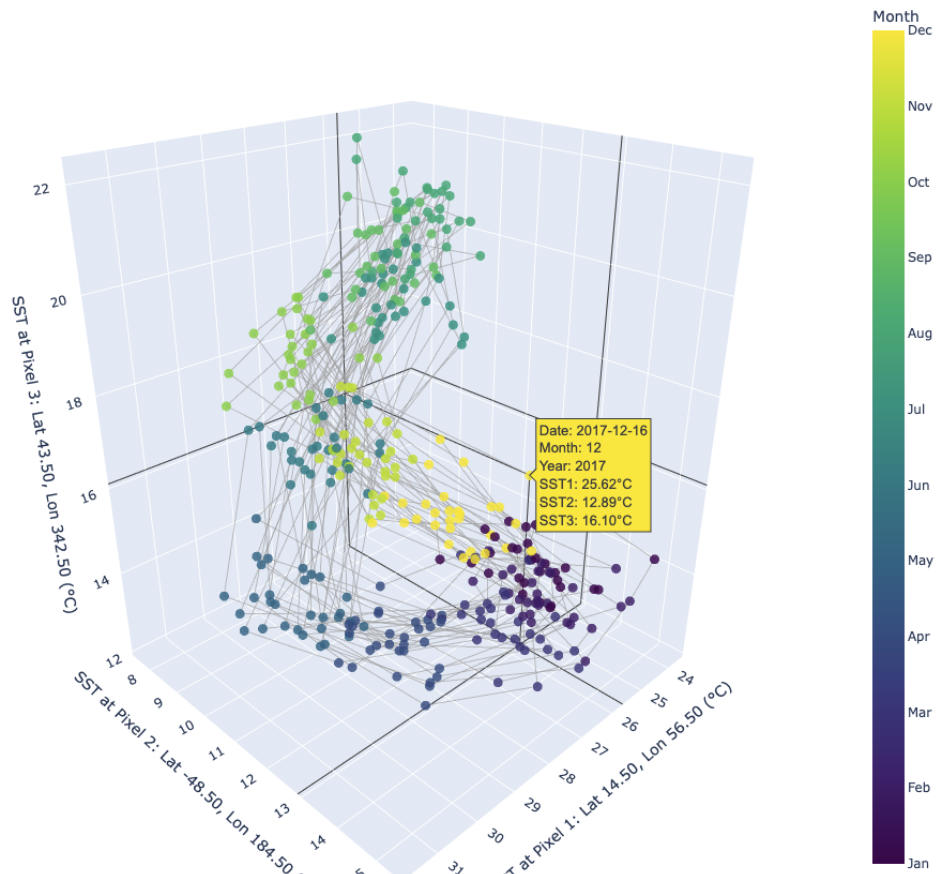


Figure 5: A 3D slice of the SST manifold used to train cBottle, the years 1991 to 2021 are shown. Because of the high density of interpolated values (here denoted by thin grey lines), we expect gradients obtained in an SST change direction corresponding to seasonal SST changes to be sensible. The same cannot be said for directions pointing away from the manifold, which most of them will be.